



HAL
open science

The ErpA/NfuA complex builds an oxidation-resistant Fe-S cluster delivery pathway

Beatrice Py, Catherine Gerez, Allison Huguenot, Claude Vidaud, Marc Fontecave, Sandrine Ollagnier de Choudens, Frédéric Barras

► To cite this version:

Beatrice Py, Catherine Gerez, Allison Huguenot, Claude Vidaud, Marc Fontecave, et al.. The ErpA/NfuA complex builds an oxidation-resistant Fe-S cluster delivery pathway. *Journal of Biological Chemistry*, 2018, 293 (20), pp.7689 - 7702. 10.1074/jbc.RA118.002160 . hal-01915442

HAL Id: hal-01915442

<https://amu.hal.science/hal-01915442>

Submitted on 12 Nov 2018

HAL is a multi-disciplinary open access archive for the deposit and dissemination of scientific research documents, whether they are published or not. The documents may come from teaching and research institutions in France or abroad, or from public or private research centers.

L'archive ouverte pluridisciplinaire **HAL**, est destinée au dépôt et à la diffusion de documents scientifiques de niveau recherche, publiés ou non, émanant des établissements d'enseignement et de recherche français ou étrangers, des laboratoires publics ou privés.



Distributed under a Creative Commons Attribution 4.0 International License

The ErpA/NfuA complex builds an oxidative resistant Fe-S cluster delivery pathway

Béatrice Py^{1,2,3*}, Catherine Gerez^{4,5,6}, Allison Huguenot^{1,2,3}, Claude Vidaud⁷, Marc Fontecave⁸, Sandrine Ollagnier de Choudens^{4,5,6}, Frédéric Barras^{1,2,3*}

From the ¹ Institut de Microbiologie de la Méditerranée, Marseille, France; ² CNRS UMR 7283, LCB, 31 Chemin Joseph Aiguier, 13009 Marseille, France; ³ Aix-Marseille Université, Marseille, France; ⁴ Université Grenoble Alpes, Grenoble, France; ⁵ CNRS UMR 5249, LCBM, Grenoble, France; ⁶ CEA/DRF/BIG/CBM/BioCat Grenoble, France; ⁷ CEA/DRF/BIAM/ Marcoule, France; ⁸ Laboratoire de Chimie des Processus Biologiques, UMR 8229 CNRS, UPMC Univ Paris 06, Collège de France, PSL Research University, Paris, France.

Running title: *Biochemical properties of E. coli Fe-S cluster carriers*

* To whom correspondence should be addressed: Béatrice Py and Frédéric Barras: Institut de Microbiologie de la Méditerranée, CNRS UMR 7283, LCB, 31 Chemin Joseph Aiguier, 13009 Marseille, France;

py@imm.cnrs.fr

barras@imm.cnrs.fr

Key words: iron-sulfur protein, Escherichia coli, oxidative stress, protein-protein interaction, metal ion-protein interaction

ABSTRACT

Fe-S cluster containing proteins occur in most organisms wherein they assist a myriad of diverse processes from metabolism to DNA repair via gene expression and bioenergetic processes. Here we used both *in vitro* and *in vivo* methods to investigate capacity of the four Fe-S carriers, NfuA, SufA, ErpA and IscA to fulfill their targeting role under oxidative stress. Likewise, Fe-S clusters exhibited varying half-live depending on the carriers they are bound to: NfuA-bound FeS cluster was more stable ($t_{1/2}$ 100 min) than SufA- ($t_{1/2}$ 55 min), ErpA ($t_{1/2}$ 54 min), and IscA ($t_{1/2}$ 45 min). Surprisingly, presence of NfuA further enhanced stability of the ErpA-bound cluster to $t_{1/2}$ 100 min. Using genetic and plasmon surface resonance analyses, we showed that NfuA and ErpA interacted directly with client proteins whereas IscA/SufA did not. Moreover, NfuA and ErpA interacted one with the other. Given all these observations we propose an architecture of the the Fe-S delivery network in which ErpA is the last factor that delivers cluster directly to most if not all client proteins. NfuA is proposed to assist

ErpA under severe unfavorable conditions. Comparison with the strategy employed in yeast and eukaryotes is discussed.

Fe-S clusters rank among the oldest cofactors, and they are surmised to have been key factors for life origin and evolution (1, 2). The first Fe-S proteins identified, by their electron paramagnetic signature, were those of mitochondrial respiratory complexes (3). In the following decades biophysical and structural approaches revealed the great variety of Fe-S cluster proteins, while genomic analyses showed their widespread adoption in living organisms (4). Nowadays, in organisms Fe-S cluster proteins participate to respiration, biosynthesis of cell building blocks and cofactors, central metabolism, gene regulation, tRNA modification, DNA synthesis and repair (5).

In vitro studies revealed that, in favorable conditions, Fe-S clusters can form spontaneously on apo-proteins clients (6, 7). However, in the 90's, studies initiated on nitrogenase maturation revealed that *in vivo* Fe-S cluster assembly requires multiproteins systems : the NIF system

dedicated to nitrogenase maturation, and two general systems, ISC and SUF, which mature most, if not all, cellular Fe-S proteins (8–10). Components of the ISC and SUF systems are conserved throughout eukaryotes and prokaryotes. In eukaryotes, the ISC and SUF Fe-S machineries are located in mitochondria and chloroplasts, respectively (11, 12).

Fe-S cluster biogenesis proceeds in two steps, assembly and delivery. The former takes place on a scaffold protein, which allows sulfur and iron to meet and combine in a Fe-S cluster. Sulfur is produced via the catalytic degradation of L-cysteine by cysteine desulfurase, whereas the molecular source of iron remains elusive. The delivery relies on a series of Fe-S carriers that transport scaffold-bound clusters to the apo-clients. Numerous Fe-S carriers have been identified in both prokaryotes and eukaryotes. These include so-called A-type carriers (ATC), named IscA, SufA and ErpA in prokaryotes and ISA1, ISA2 in eukaryotes (13–17). Others carriers include the P-loop NTPases, (Ind1 in mitochondria, ApcC in *Salmonella*) (18–21), the monothiol glutaredoxins (Grx 5 in yeast and GrxD in *E. coli*) (22–24) and the highly conserved NFU-type proteins that have been shown to interact with target proteins (25–33).

Understanding how Fe-S clusters are delivered to the large number of functionally and structurally diverse Fe-S cluster proteins is a challenging task. Indeed, in most organisms, clients are actually a set of structurally and functionally diverse protein species and it is difficult to think of a common maturation pathway shared by all of them. Moreover, Fe-S clusters are highly sensitive to environmental changes and, in particular, can be destabilized by reactive oxygen species (ROS) depending upon their solvent accessibility on the host protein (34–36). Last, Fe-S clusters arise under different structure, i.e. 2Fe-2S, 3Fe-4S, 4Fe-4S or in more complex association with other metal and cofactors (1). How organisms keep on inserting clusters in such a great diversity of substrates and conditions and whether all Fe-S proteins get their clusters delivered by the same set of factors is a daunting issue.

Multiple parameters can be foreseen as controlling the delivery process: (i) genetically controlled level of delivery factors available in a given condition, (ii) affinity between delivery factors and apo-targets, and (iii) intrinsic biochemical features of delivery factors. Our previous study had illustrated how genetic regulation orchestrated the choice of routes Fe-S clusters take to reach essential enzymes, IspG/H, and the two transcriptional factors, IscR and NsrR, throughout fluctuating conditions (16, 37). The present study provides key findings on the two other parameters and provides us with an unprecedented view of Fe-S cluster trafficking and delivery.

We investigated the intrinsic capacity of IscA, SufA, ErpA and NfuA, to stabilize bound Fe-S cluster exposed to aerobic conditions. We proceeded by analyzing the contribution of each of them into the maturation of a series of Fe-S enzymes, including IspG and IspH, two essential Fe-S enzymes involved in the production of isoprenoids (38, 39). This provided us for the first time with a direct ranking of the Fe-S cluster carriers according to their intrinsic capacity to resist ROS potential damages. Another key finding was the observation of a privileged partnership between ErpA and NfuA, providing the cell with a new type of “hybrid” carrier, the Fe-S cluster of which exhibited the highest level of resistance to ROS. Altogether this allowed us to propose a model of the Fe-S cluster delivery network that predict ErpA to be in charge of the maturation of most if not all Fe-S enzymes. Its closer association with NfuA appears as a new strategy for the cell to meet with transiently occurring destabilizing conditions.

Results

NfuA is required for IspG/H maturation under oxidative stress

Earlier, we found that growth of the *E. coli* $\Delta nfuA$ mutant on rich medium is severely affected in the presence of paraquat (PQ), a superoxide radical generator (25). Our previous analysis informed us that such a phenotype is likely due to an insufficient amount of

isopentenylphosphate IPP, due to a poor maturation of IspG and IspH, two Fe-S cluster containing enzymes (17). Therefore we tested whether the NfuA protein contributes to the Fe-S cluster delivery route towards maturation of IspG/H. For this, we introduced the eukaryotic IPP biosynthesis (Fe-S)-independent pathway - referred as the mevalonate pathway (MVA)- in the $\Delta nfuA$ mutant and found that ectopic expression of this pathway was sufficient to rescue viability of the *nfuA* mutant (Fig. 1). This result indicated that NfuA is required for Fe-S cluster delivery to IspG/H under oxidative stress.

NfuA interacts with ErpA

To know if NfuA cooperates with the ATC, we tested the interaction of NfuA with the ATC using the bacterial two-hybrid system. NfuA/ErpA interaction was observed as the BTH101 cells synthesizing the T18-NfuA and T25-ErpA hybrid proteins (pT18-NfuA, pT25-ErpA) exhibited β -galactosidase activity (Fig. 2A). In contrast, no interaction was indicated between NfuA and IscA or between NfuA and SufA using this assay (Fig. 2A). ErpA/NfuA interaction was also tested by surface plasmon resonance (SPR) using apo-proteins. Purified NfuA was immobilized onto a Biacore sensor CM5 chip and ErpA was serially diluted and injected. The calculated dissociation constant (Kd) of the ErpA/NfuA interaction was determined to be $48.5 \pm 0.5 \mu\text{M}$ (Fig. 2B). In contrast, no interaction was observed between NfuA and SufA or IscA (data not shown). Taken together these analyses revealed that NfuA and ErpA physically interact with each other, and suggest they might partner to form a discrete path within the Fe-S cluster delivery network.

Unidirectional Fe-S cluster transfer from NfuA to ErpA

To test if Fe-S cluster transfer occurs between ErpA and NfuA, an *in vitro* test was used. Holo-NfuA contains a 4Fe-4S per dimer and ErpA is able to bind 2Fe-2S cluster per monomer (17, 25, 26, 40). His-tagged holo-NfuA (1.2 ± 0.1 Fe and 1 ± 0.2 S/monomer; inset Fig. 3A) was incubated, under anaerobic conditions, with one

equivalent of untagged apo-ErpA, for 1 hour. After separation by chromatography onto a Ni-NTA column, iron and sulfide contents of each protein were analyzed. ErpA contained 1 ± 0.1 Fe and 0.7 ± 0.2 S/monomer and its visible spectrum was characteristic of a 2Fe-2S cluster protein with absorption bands at 420 nm and 320 nm. On the contrary, NfuA had lost its 420 nm Fe-S cluster absorption band and contained less than 0.1 Fe and S/monomer (Fig. 3A). In a separate experiment, holo-ErpA was incubated with apo-NfuA, and the two entities submitted to same analyses as described above after separation. No modification either in iron/sulfide content or in spectrum was observed before and after co-incubation (Fig. 3B). Together, these analyses showed that, *in vitro*, an unidirectional Fe-S cluster transfer occurs from NfuA to ErpA.

Stability of Fe-S cluster to oxidative damages varies with carrier identity

In vivo studies showed that ErpA and NfuA are required for Fe-S cluster transfer under aerobiosis and oxidative stress, respectively. Therefore, we tested the stability of Fe-S clusters bound to NfuA and to ErpA when exposed to O₂. Before exposure to O₂, reconstituted holo-NfuA contained 1.4 ± 0.2 Fe molecules per monomer and displayed a 4Fe-4S cluster-characteristic UV-visible spectrum in agreement with published data (40) (Fig. 4A). The degradation of the Fe-S cluster was monitored by the absorbance variation at 420_{nm} as a function of time when diluted into oxygenated buffer containing controlled amount of O₂. Under these conditions the half-life of the NfuA Fe-S cluster was 100 ± 10 minutes (Fig. 4A). Holo-ErpA exhibited a 2Fe-2S cluster-characteristic UV-visible spectrum (Fig. 4B). Upon controlled O₂ exposure, half-life of its cluster was 54 ± 3 minutes, (Fig. 4B). We also tested the stability of the Fe-S cluster of two other ATC, IscA and SufA under the same experimental conditions, and found half-lives of 45 ± 4 and 55 ± 7 minutes, respectively (Fig. 4C). All together, these results showed that Fe-S cluster bound to diverse carriers exhibit different capacities to resist oxidative damages with the

decreasing stability order NfuA > ErpA = SufA > IscA.

The NfuA/ErpA-bound cluster has an increased stability

Last, we tested whether stability of the ErpA bound Fe-S cluster was modified in the presence of NfuA. Both apo-NfuA and holo-ErpA proteins were mixed and exposed to O₂, as above. Half-life of the Fe-S cluster bound to ErpA reached 90 +/- 6 minutes, that is, an enhancement by two-fold as compared with Fe-S bound to ErpA alone (Fig. 5). Thus, our results indicated that the NfuA somehow allowed ErpA bound Fe-S cluster to enhance its stability towards O₂.

NfuA and ErpA interact directly with the client proteins IspG and IspH

SPR was used to test the interaction between IspG/H and the Fe-S carriers. For the experiments performed with IspG, serially diluted IspG was injected into sensor chips coated with NfuA, or with ErpA. The sensorgrams showed binding of IspG to both NfuA and ErpA (Fig. 6). Global evaluation using the 1:1 Langmuir binding model yielded K_d values of 22.5 +/- 0.5 μM for the IspG/ErpA interaction and of 30 +/- 2 μM for the IspG/NfuA interaction.

For the experiments performed with IspH, serially diluted NfuA or ErpA were injected into IspH coated sensor chips. Even though sensorgrams showed binding of NfuA and ErpA to IspH, the maximum response (R_{max}), was unattainable preventing determination of a K_d value (data not shown). We also used bacterial two-hybrid approach in order to detect this interaction between NfuA, ErpA and IspH. We showed that the BTH101 cells synthesizing T18-IspH and T25-NfuA hybrid proteins exhibited β-galactosidase activity, indicating an IspH/NfuA interaction (Fig. 7A). In addition, the two-hybrid system allowed us to show that the N-terminal domain of NfuA was sufficient to mediate the interaction with IspH (Fig. 7B). An interaction, albeit weak, was also observed between IspH and ErpA (Fig. 7A). In contrast, no interaction was observed between IspH and SufA or IscA (Fig. 7A).

Collectively, these results indicated that NfuA and ErpA are able to interact directly with the client IspG and IspH proteins.

Both ErpA and NfuA are required for the maturation of aconitase B and the respiratory complexes I and II

Our previous study revealed a role of NfuA in the maturation of AcnB and the respiratory complex I (Fig. S1) (40). We then asked whether ErpA participates to the maturation of these Fe-S cluster-containing proteins.

First, we assayed the AcnB activity in the conditional mutant in which the expression of the *erpA* gene was under arabinose induction and glucose repression referred to as LL401 (*ara_p::erpA*), in which the $\Delta acnA$ mutation has been introduced (BP721) (17). ErpA depleted cells were obtained after 2 hours growth in glucose-supplemented medium (Fig. 8). In the ErpA depleted cells, aconitase activity was decreased by 80% when compared to the ErpA replete cells grown in the presence of arabinose, while AcnB was detected at an identical level in both ErpA-repleted and -depleted cells (Fig. 8). The NfuA protein level was slightly increased in ErpA-depleted cells (Fig. S2). SPR was used to investigate the interaction between ErpA and AcnB. Serially diluted ErpA (0-270 μM), was injected into sensor chips coated with AcnB (Fig. S3A). The K_d value for the ErpA/AcnB interaction was 50 +/- 5 μM. We also used SPR experiments to quantify the previously shown NfuA-AcnB interaction (40). Serially diluted NfuA (0-160 μM) injected into sensor chips coated with AcnB yielded to a K_d value of 29 +/- 3 μM (Sup data, Fig. S3B).

We then tested whether ErpA was also required for the maturation of complex I. ErpA depleted cells of the LL401 strain exhibited a drastic decrease (70%) for complex I activity when compared to ErpA replete cells grown in presence of arabinose (Fig. 8).

Last, we tested the contribution of ErpA and NfuA to the maturation of the respiratory complex II (Sdh). When grown in glucose, the Sdh activity of the LL401 strain was found to be drastically reduced

(85%) (Fig. 8). In the *nfuA* mutant, the Sdh activity was decreased by 35% (Fig. 9).

Collectively, all these data indicate that maturation of the respiratory complexes I and II are under the assistance of both ErpA and NfuA under aerobic conditions, and that maturation of AcnB requires ErpA under aerobic conditions, and NfuA under oxidative stress conditions.

ErpA interacts with IscA and SufA

Using the Biacore experiment, we tested whether ErpA can physically interact with the ATC of the ISC and SUF machineries, IscA and SufA, respectively. ErpA was immobilized onto a Biacore sensor CM5 chip and IscA and SufA were serially diluted and injected. A dose-response curve was obtained where an increase in response units was observed with increasing concentrations of IscA (0-200 μ M) and SufA (0-600 μ M), indicating that ErpA interacted with IscA and SufA (Fig. 10). The sensorgrams indicated that IscA and SufA were released in a short time without the necessity of chip regeneration. The calculated dissociation constant (Kd) of the ErpA/IscA and ErpA/SufA interactions was determined to be 40 +/- 3 μ M and 90 μ M +/- 2 μ M respectively. These results indicated that ErpA is able to interact with IscA and SufA.

Multicopy suppression of the nfuA growth defect by erpA

Results above evidenced NfuA and ErpA contribute to the maturation of the same set of enzymes. Therefore, we tested whether NfuA and ErpA are functionally redundant *in vivo*. For this, we made use of a multicopy-based suppression approach. A pBAD derivative plasmid expressing *erpA*, (pBAD-*erpA*), suppressed paraquat sensitivity of the *nfuA* mutant (Fig. 11). In contrast, increased *nfuA* gene dosage failed to suppress non-viability caused by *erpA* mutation under aerobiosis (Fig. 12). Last, pBAD-*iscA* and pBAD-*sufA*, plasmids expressing *iscA* and *sufA*, respectively, failed to suppress Δ *nfuA* mutant sensitivity to paraquat (Fig. 11). Altogether, these data showed that ErpA overproduction overcomes the need of NfuA for IspG/H maturation but that the converse is not true.

Discussion

Interest in Fe-S cluster biology keeps expanding as one realizes how much these cofactors are central to multiple issues, from basic knowledge to molecular medicine, antibiotic resistance and biotechnological applications (41, 42). In most organisms several dozens of structurally and functionally diverse client protein species need to acquire a Fe-S cluster for functioning. The diversity of clients, the diversity of the clusters and the fluctuating environmental conditions under which Fe-S cluster trafficking takes place make the question of the delivery a most challenging issue. Here we show that synthesizing different carriers can afford different ROS-resistance environment for transported Fe-S clusters, hence delivery circuits better adapted to sustain oxidative stress. We show that enhanced resistance to ROS can also be achieved by interaction between Fe-S carriers. We propose a model in which, right after the assembly step, Fe-S trafficking network diversifies in multiple branches, which eventually converge towards ErpA. This unprecedented view of Fe-S cluster trafficking and delivery is discussed in comparison with the eukaryotic situation.

The present study allowed us to quantitate ROS resistance capacity of a cluster bound to NfuA, ErpA, SufA and IscA carriers. Likewise, NfuA and SufA-carried clusters showed the highest resistance to ROS. This is fully consistent with the genetically based view of SufA and NfuA being stress responding factors, and predicted to be better adapted to deliver clusters under oxidative stress conditions (16, 25, 26). NfuA results from the fusion between a NFU domain, at the C-terminal region, and, at the N-terminal region, a degenerated ATC domain lacking the Fe-S cluster liganding cysteine residues (25, 26, 40). NfuA forms a dimer and binds a 4Fe-4S cluster in its NFU domain, likely at the dimer interface (25, 26, 40). Then, it is possible that the cluster stability of NfuA is related to the four cysteinyl ligations and/or shielding by the dimer formation.

An unsuspected association between NfuA and ErpA was observed both by SPR and two-hybrid based methods. This

association resulted in an enhanced stability of the ErpA bound cluster as compared when bound to ErpA alone. Next biochemical and structural studies will aim at solving the molecular basis for the enhanced ROS resistance procured by the NfuA-ErpA interaction.

Our previous phylogenetic studies permitted us to classify ATC within two different families. ErpA and IscA/SufA were classified into ATC-I and -II families, respectively (16). Members of the ATC-I family were predicted to partnership with the apo-targets, whereas the ATC-II members were thought to be connected to scaffolds (16). The present bacterial two-hybrid and SPR-based investigations fully support the phylogenetically-based functional prediction. Direct interactions were observed between apo-targets (IspG/H and AcnB) and ErpA, but not IscA and/or SufA (data not shown). Taken together with our previous genetic analysis, this observation comforts the view that scaffold-bound Fe-S clusters are transferred to ATC-II, IscA or SufA, which transfer them to ErpA, which delivers them to the apo-targets. In mitochondria, once assembled by the core biogenesis machinery, 2Fe-2S clusters reach a heteromeric platform, the ISCA1-ISCA2-Iba57 complex, which converts them into 4Fe-4S before to target them to a so-called dedicated factors, which in turn allow maturation of cellular Fe-S proteins (15, 43–45). Mammalian ISCA1/2 proteins contain 2Fe-2S clusters. Heterodimer ISCA1-ISCA2 can assemble 4Fe-4S cluster in the presence of GRX5 implying that the heterodimeric complex is the functional unit for 4Fe-4S cluster formation before their transfer to specific targets (45). ISCA1 is an ATC-II, like IscA and SufA, while ISCA2 is an ATC-I, like ErpA. In essence therefore, the complex ISCA1-ISCA2 resembles the partnership IscA/ErpA or SufA/ErpA discussed above. The difference though is that no stable bacterial ATCII-ATCI complex has ever been isolated and two-hybrid based methods failed to reveal any interaction. Note however that in mice, despite forming a complex, ISCA1 and ISCA2 are able to carry out separate tasks, presumably depending upon the substrates and the conditions (46).

Both NfuA and ErpA exhibit related affinity for Fe-S client proteins; the K_d value of the ErpA/IspG (23 μ M) and NfuA/IspG (28 μ M) interactions are within a similar range like were those for the interaction between AcnB and ErpA (50 μ M) or NfuA (29 μ M). A K_d value of 44 μ M was reported for the interaction of NfuA with MiaB, involved in tRNA modification (32). Thus, like ErpA, NfuA appears to have all features required to interact directly with targets, and could be positioned at the ultimate step within the Fe-S cluster delivery process. If direct transfer between NfuA and target proteins can occur *in vivo*, its contribution appears very modest regarding the contribution of ErpA. Hence, lack or depletion of ErpA caused a stronger phenotype than the lack of NfuA. The *erpA* gene is crucial for both anaerobic and aerobic respiration as shown here by a drop in complexes I and II activities by over 70% and 85%, whereas, a *nfuA* mutant exhibited a less than 2-fold reduction in Complex I and Complex II activities. Similarly, aconitase B activity was down by over 80% in ErpA-depleted cells whereas it was only slightly altered under stress conditions in cells lacking NfuA. Also, *erpA* was able to act as multicopy suppressors of *nfuA*, while the reverse was not true. We thus favor the hypothesis that in *E. coli*, NfuA act conjointly with ErpA, by providing it a Fe-S cluster, rather being an ultimate Fe-S donor for target proteins (Fig. 13).

The yeast and human Nfu1 and the *E. coli* NfuA proteins share a conserved NFU-type C-terminal domain that binds a 4Fe-4S cluster. Interestingly, as NfuA, the yeast and human Nfu1 were found associated with the ISA proteins (33, 46). In yeast, defects exhibited by *nfu1* mutation were of much lesser extent than those caused by mutations in the ISA complex (ISCA homologs in yeast) complex (13, 14, 30, 47). In fact, defects were mainly apparent under oxidative stress conditions (33, 47). Hence, the parallel with the *E. coli* situation is striking. Moreover, overexpression of Isa2, which we classified as an ATC-I member, was able to suppress defect of *NFU1* mutant whereas overexpression of Isa1, an ATC-II member failed to do so (33). This is highly

reminiscent of what we observed here with *E. coli*, wherein *erpA*, an ATC-I, but not *iscA* or *sufA*, both ATC-II members, was able to act as multicopy suppressors of *nfuA*. This argues that in both prokaryotes and eukaryotes NFU-containing proteins are called upon in stress conditions at the delivery step, but that their contribution can be by-passed given that the level of ATC-II member (ISCA2 or *ErpA*) is sufficiently high, and that the proposed scenario of NFU proteins as a Fe-S refuel for ATC-I can also be envisioned at the late stage of the mitochondrial Fe-S delivery step.

In conclusion, independently of the organisms considered and of the type of Fe-S client proteins to be matured, a same overall strategy has been retained throughout evolution. Despite the multitude of apo-protein clients waiting for their clusters, cells evolved a hand-full of carriers, which they either synthesize at appropriate levels under a set of conditions, or combine in different higher-order organization, from homodimers to heterotetramers, each possibility providing a better solution to adapt to the diversity of client proteins and growth conditions. This study pinpoints how diversifying carriers, and combining different carriers, constitute two strategies the cell evolved to yield multiple delivery pathways in particular a robust ROS resistant delivery network.

Experimental procedures

Strains and growth conditions

Strains used in this study are listed in Table 1. The $\Delta acnA::kan$ KEIO mutation was introduced by P1 transduction (48). *E. coli* strains were grown in Luria-Bertani (LB) rich medium at 37°C. Solid media contained 1.5% agar. Ampicillin was used at 50 μ g/ml. Arabinose (0.2%), and mevalonate (1 mM) were added when required.

Paraquat sensitivity Test

Paraquat sensitivity test was performed on overnight cultures that were diluted in sterile PBS and directly spotted onto LB plates containing 100 μ M paraquat (25). The plates were incubated overnight at 37°C before growth was scored.

Plasmids construction

Construction of plasmids pT18-NfuA, pT25-NfuA, pT25-ATC* was described previously. (40). Plasmids pT25-ErpA, pT25-IscA, pT25-SufA and pT18-IspH were constructed by, first, PCR amplification from the MG1655 chromosomal DNA using 2HErpAup/2HErpAado, 2HIscAup/2HIscAado 2HSufAup/2HSufAado and 2HIspHup/2HIspHdo primers pairs. The *erpA*-, *ispH*-containing PCR fragments were digested by *EcoRI PstI* enzymes, and the *iscA*-, *sufA*-containing PCR fragments were digested by the *PstI KpnI* enzymes. All the constructs obtained by PCR-fragment cloning were checked by DNA sequencing.

Protein purification

Apo-NfuA, -ErpA, SufA, and -IscA, were obtained as previously described (25, 49). Aconitase B was purified as described for aconitase A (50). Purification of IspG-His was performed as described in (17) and IspH was a gift of M. Seeman (IC, Strasbourg).

Surface plasmon resonance analysis

The binding studies were performed using Biacore™ T200 instrument and CM5 sensor chips. Proteins were covalently immobilized onto the chip using a standard primary amine coupling procedure. The same amine coupling procedure, but without any protein, was performed on the reference channel as a blank to subtract any non-specific binding signal. The analytes, dissolved in running Tris buffer (Tris 50 mM, NaCl 150 mM at pH 7.4), or HBS buffer (Hepes 10 mM, NaCl 150 mM, EDTA 3 mM, Tween 0,005% at pH 7.4) were serially diluted to various concentrations with the running buffer. According to their kinetics of association and dissociation, they were injected for 50 to 125 seconds during the association phase at a constant flow rate of 10 μ l/min at 25°C. The dissociations were subsequently followed for 75 to 250 seconds at the same flow rate. For each cycle the sensor surface was regenerated with 10 mM Gly-HCl buffer (pH 2.0) when the data collection was finished. To calculate the rate and affinity constants the results from the sensograms were fit globally with BIAcore 3000 analysis software

(BIAevaluation Version 4.1) that propose 1:1 Langmuir binding modes.

Bacterial two-hybrid

We used the adenylate cyclase-based two-hybrid technique (51). DNA inserts encoding the proteins of interest were obtained by PCR and were cloned into pUT18C and pKT25 plasmids. After co-electroporation of the BTH101 strain with the two plasmids expressing the hybrid proteins, plates were incubated at 30°C for 2 days. Three milliliters of LB medium supplemented with antibiotics and IPTG at the recommended concentration (51) were inoculated and incubated overnight at 30°C. β -Galactosidase activity was determined as described by Miller (1992).

***In vitro* Fe-S reconstitution**

NfuA and the three ATC were reconstituted as described (25, 52). The purified proteins were obtained primarily in the apo-form, and were reconstituted anaerobically in the glove box at 18°C as follows: 0.08 mM protein was mixed with 5 mM DTT, 10 μ M IscS, 1 mM L-cysteine and 0.2 mM ferrous iron in 50 mM Tris pH 8, 50 mM KCl. After 1h30 incubation, samples were passed over a desalting column and concentrated when needed.

Cluster transfer

All the following procedures were performed anaerobically in the glove box at 18°C. Fe-S cluster transfer from holo-ErpA to apo-NfuA. Apo-NfuA_{his} (75 μ M) was mixed for 1 h with holo-ErpA (reconstituted ErpA as described above) in buffer A (0.1 M Tris-HCl pH 8, 50 mM KCl, 5 mM DTT) in a molar ratio to give sufficient amounts of iron and sulfur per NfuA monomer. After incubation, DTT was removed from the solution on a Nap-10 column equilibrated with buffer B (0.1 M Tris-HCl pH 8, 0.1 M NaCl) prior to separation of the proteins on a Ni-NTA affinity column (1 ml) equilibrated with the same buffer. Fe-S donor proteins, which do not contain a poly histidine tag, were recovered in the flow-through and wash fractions, while NfuA_{his} was eluted with buffer B containing 0.2 M imidazole and desalted over a Nap-10 column to remove imidazole. Each fraction (wash and

elution fractions) was analyzed for its Fe content, and a UV-visible spectrum was recorded.

Fe-S cluster transfer from holo-NfuA to apo-ErpA. Apo-ErpA was first pre-reduced with 5 mM DTT for 10 min. DTT was removed over onto a MicroBio-Spin 6 chromatography column. Reduced ErpA (150 μ M) and holo-NfuA_{his} were mixed together in buffer B, in a molar ratio allowing to provide one iron and one sulfur atoms per ErpA monomer. After 1 h incubation, proteins were separated on the Ni-NTA affinity column and analyzed as described above.

Protein analysis

Protein concentrations were measured by the method of Bradford using bovine serum albumin as a standard. Iron and sulfide quantifications were carried out as previously described (53, 54). UV-visible (UV-vis) spectra were recorded on a Cary Bio (Varian) spectrophotometer.

Fe-S cluster stability towards oxygen

To control the amount of oxygen that would react with the reconstituted proteins Fe-S cluster, the experiment was performed using a cuvette containing 100 μ L of a solution (0.1 M Tris, 0.1 M KCl at pH 8) equilibrated with air outside the glove box. At 20 °C and at 760 mmHg, this solution contains 284 μ M oxygen (55). The cuvette was sealed with a septum and introduced into the glove box. Controlled amount of the reconstituted proteins were introduced into the cuvette using a Hamilton syringe to give a ratio 1/20 for (amount Fe)/O₂. The kinetics of degradation of the Fe-S cluster was followed by UV-vis spectroscopy.

Enzymatic activity

Aconitase activity. Strains were grown in LB at 37°C to an OD600 of 0.8. The cells were harvested, washed with 50 ml of 50 mM Tris-HCl pH 7.5 buffer, frozen in liquid nitrogen and stored at -80°C. The cell pellets were transferred to a Coy anaerobic chamber (90% N₂, 10% H₂), and resuspended in anaerobic 50 mM Tris-HCl pH 7.5 (0.4% of the culture volume). Cells were lysed using a French press, and centrifuged at 16 000g for 5 min.

Supernatant was immediately frozen in liquid nitrogen. In the Coy anaerobic chamber, cell extracts containing 100 mg of protein were added to 50 mM Tris-HCl pH 7.5, 0.6 mM MnCl₂, 30 mM citrate, 0.2 mM NADP⁺, 1.7 U of isocitrate dehydrogenase in a 1 ml final volume. Aconitase activity was assayed by following the formation of NADPH in the coupled assay as an increase in absorbance at 340 nm (56).

NADH dehydrogenase activity. NADH dehydrogenase activity was adapted from described (57). Briefly, cells were harvested by centrifugation, resuspended in 50mM phosphate buffer pH 7.5, lysed using a French press and frozen immediately in liquid nitrogen. NADH activity was assayed on the thawed samples, by immediately adding D-NADH (200 mM) as substrate and by following A₃₄₀.

Succinate dehydrogenase activity. Cells were harvested by centrifugation, resuspended in buffer 50mM phosphate buffer pH 7.5 and lysed using a French

press. Following centrifugation (15 000 r.p.m. for 2h at 4°C) the supernatant was submitted to ultracentrifugation (45 000 r.p.m. for 2h at 4°C). SDH activity was assayed on the pellet fraction resuspended in 50mM phosphate buffer pH 7.5. Sample were pre-incubated 30 min at 30°C in 4mM succinate, 1mM KCN, 50mM phosphate buffer pH 7,5. Assay was performed by adding DCPIP (Dichlorophenolindophenol) (100mM) and PES (Phenazine ethosulfate) (1 mM) as substrate and by following A₆₀₀.

Immunoblotting procedure

Equal quantities of proteins were separated on SDS-PAGE acrylamide gels and transferred onto nitrocellulose membranes. The membrane filter was incubated with appropriate antibodies (anti-AcnB, anti-ErpA) diluted 1/2000. Immunoblots were developed by using horseradish peroxidase-conjugated goat anti-rabbit antibody, followed by chemiluminescence detection.

Acknowledgements

We thank all members of the FB group for fruitful discussions. Thanks are due to Béatrice Roche for construction of the *ara_p::erpA ΔacnA* strain (BP721). Thanks are due to Olivier Averseng for his advices and technical assistance for SPR experiments. This work was supported by grants from the CNRS, the ANR (FeStress), the Institut Universitaire de France, the CEA, the Aix-Marseille Université, and the Université Joseph Fourier.

Conflict of interest: The authors declare that they have no conflicts of interest with the contents of this article.

References

1. Beinert, H. (2000) Iron-sulfur proteins: ancient structures, still full of surprises. *J. Biol. Inorg. Chem. JBIC Publ. Soc. Biol. Inorg. Chem.* **5**, 2–15
2. Milner-White, E. J., and Russell, M. J. (2005) Sites for phosphates and iron-sulfur thiolates in the first membranes: 3 to 6 residue anion-binding motifs (nests). *Orig. Life Evol. Biosphere J. Int. Soc. Study Orig. Life.* **35**, 19–27
3. Beinert, H., and Sands, R. (1960) Studies on mitochondria and submitochondrial particules by paramagnetic resonance (EPR) spectroscopy. *Biochem. Biophys. Res. Commun.*
4. Andreini, C., Rosato, A., and Banci, L. (2017) The Relationship between Environmental Dioxygen and Iron-Sulfur Proteins Explored at the Genome Level. *PLoS One.* **12**, e0171279
5. Py, B., and Barras, F. (2010) Building Fe-S proteins: bacterial strategies. *Nat. Rev. Microbiol.* **8**, 436–446
6. Malkin, R., and Rabinowitz, J. C. (1966) The reconstitution of clostridial ferredoxin. *Biochem. Biophys. Res. Commun.* **23**, 822–827
7. Hagen, K. S., Reynolds, J. G., and Holm, R. H. (1981) Definition of reaction sequences resulting in self-assembly of [Fe₄S₄(SR)₄]²⁻ clusters from simple reactants. *J. Am. Chem. Soc.* **103**, 4054–4063
8. Roche, B., Aussel, L., Ezraty, B., Mandin, P., Py, B., and Barras, F. (2013) Iron/sulfur proteins biogenesis in prokaryotes: formation, regulation and diversity. *Biochim. Biophys. Acta.* **1827**, 455–469
9. Boyd, E. S., Thomas, K. M., Dai, Y., Boyd, J. M., and Outten, F. W. (2014) Interplay between oxygen and Fe-S cluster biogenesis: insights from the Suf pathway. *Biochemistry (Mosc.).* **53**, 5834–5847
10. Blanc, B., Gerez, C., and Ollagnier de Choudens, S. (2015) Assembly of Fe/S proteins in bacterial systems: Biochemistry of the bacterial ISC system. *Biochim. Biophys. Acta.* **1853**, 1436–1447
11. Braymer, J. J., and Lill, R. (2017) Iron-sulfur cluster biogenesis and trafficking in mitochondria. *J. Biol. Chem.* **292**, 12754–12763
12. Balk, J., and Schaedler, T. A. (2014) Iron cofactor assembly in plants. *Annu. Rev. Plant Biol.* **65**, 125–153
13. Pelzer, W., Mühlenhoff, U., Diekert, K., Siegmund, K., Kispal, G., and Lill, R. (2000) Mitochondrial Isa2p plays a crucial role in the maturation of cellular iron-sulfur proteins. *FEBS Lett.* **476**, 134–139
14. Kaut, A., Lange, H., Diekert, K., Kispal, G., and Lill, R. (2000) Isa1p is a component of the mitochondrial machinery for maturation of cellular iron-sulfur proteins and requires conserved cysteine residues for function. *J. Biol. Chem.* **275**, 15955–15961
15. Sheftel, A. D., Wilbrecht, C., Stehling, O., Niggemeyer, B., Elsässer, H.-P., Mühlenhoff, U., and Lill, R. (2012) The human mitochondrial ISCA1, ISCA2, and IBA57 proteins are required for [4Fe-4S] protein maturation. *Mol. Biol. Cell.* **23**, 1157–1166
16. Vinella, D., Brochier-Armanet, C., Loiseau, L., Talla, E., and Barras, F. (2009) Iron-sulfur (Fe/S) protein biogenesis: phylogenomic and genetic studies of A-type carriers. *PLoS Genet.* **5**, e1000497
17. Loiseau, L., Gerez, C., Bekker, M., Ollagnier-de Choudens, S., Py, B., Sanakis, Y., Teixeira de Mattos, J., Fontecave, M., and Barras, F. (2007) ErpA, an iron sulfur (Fe S) protein of the A-type essential for respiratory metabolism in Escherichia coli. *Proc. Natl. Acad. Sci. U. S. A.* **104**, 13626–13631
18. Bych, K., Kerscher, S., Netz, D. J. A., Pierik, A. J., Zwicker, K., Huynen, M. A., Lill, R.,

- Brandt, U., and Balk, J. (2008) The iron-sulphur protein Ind1 is required for effective complex I assembly. *EMBO J.* **27**, 1736–1746
19. Sheftel, A. D., Stehling, O., Pierik, A. J., Netz, D. J. A., Kerscher, S., Elsässer, H.-P., Wittig, I., Balk, J., Brandt, U., and Lill, R. (2009) Human ind1, an iron-sulfur cluster assembly factor for respiratory complex I. *Mol. Cell. Biol.* **29**, 6059–6073
20. Boyd, J. M., Pierik, A. J., Netz, D. J. A., Lill, R., and Downs, D. M. (2008) Bacterial ApbC can bind and effectively transfer iron-sulfur clusters. *Biochemistry (Mosc.)*. **47**, 8195–8202
21. Boyd, J. M., Lewis, J. A., Escalante-Semerena, J. C., and Downs, D. M. (2008) Salmonella enterica requires ApbC function for growth on tricarballoylate: evidence of functional redundancy between ApbC and IscU. *J. Bacteriol.* **190**, 4596–4602
22. Rodríguez-Manzanique, M. T., Tamarit, J., Bellí, G., Ros, J., and Herrero, E. (2002) Grx5 is a mitochondrial glutaredoxin required for the activity of iron/sulfur enzymes. *Mol. Biol. Cell.* **13**, 1109–1121
23. Picciocchi, A., Saguez, C., Boussac, A., Cassier-Chauvat, C., and Chauvat, F. (2007) CGFS-type monothiol glutaredoxins from the cyanobacterium Synechocystis PCC6803 and other evolutionary distant model organisms possess a glutathione-ligated [2Fe-2S] cluster. *Biochemistry (Mosc.)*. **46**, 15018–15026
24. Bandyopadhyay, S., Gama, F., Molina-Navarro, M. M., Gualberto, J. M., Claxton, R., Naik, S. G., Huynh, B. H., Herrero, E., Jacquot, J. P., Johnson, M. K., and Rouhier, N. (2008) Chloroplast monothiol glutaredoxins as scaffold proteins for the assembly and delivery of [2Fe-2S] clusters. *EMBO J.* **27**, 1122–1133
25. Angelini, S., Gerez, C., Ollagnier-de Choudens, S., Sanakis, Y., Fontecave, M., Barras, F., and Py, B. (2008) NfuA, a new factor required for maturing Fe/S proteins in Escherichia coli under oxidative stress and iron starvation conditions. *J. Biol. Chem.* **283**, 14084–14091
26. Bandyopadhyay, S., Naik, S. G., O'Carroll, I. P., Huynh, B.-H., Dean, D. R., Johnson, M. K., and Dos Santos, P. C. (2008) A proposed role for the Azotobacter vinelandii NfuA protein as an intermediate iron-sulfur cluster carrier. *J. Biol. Chem.* **283**, 14092–14099
27. Tong, W.-H., Jameson, G. N. L., Huynh, B. H., and Rouault, T. A. (2003) Subcellular compartmentalization of human Nfu, an iron-sulfur cluster scaffold protein, and its ability to assemble a [4Fe-4S] cluster. *Proc. Natl. Acad. Sci. U. S. A.* **100**, 9762–9767
28. Léon, S., Touraine, B., Ribot, C., Briat, J.-F., and Lobréaux, S. (2003) Iron-sulphur cluster assembly in plants: distinct NFU proteins in mitochondria and plastids from Arabidopsis thaliana. *Biochem. J.* **371**, 823–830
29. Mashruwala, A. A., Pang, Y. Y., Rosario-Cruz, Z., Chahal, H. K., Benson, M. A., Mike, L. A., Skaar, E. P., Torres, V. J., Nauseef, W. M., and Boyd, J. M. (2015) Nfu facilitates the maturation of iron-sulfur proteins and participates in virulence in Staphylococcus aureus. *Mol. Microbiol.* **95**, 383–409
30. Navarro-Sastre, A., Tort, F., Stehling, O., Uzarska, M. A., Arranz, J. A., Del Toro, M., Labayru, M. T., Landa, J., Font, A., Garcia-Villoria, J., Merinero, B., Ugarte, M., Gutierrez-Solana, L. G., Campistol, J., Garcia-Cazorla, A., Vaquerizo, J., Riudor, E., Briones, P., Elpeleg, O., Ribes, A., and Lill, R. (2011) A fatal mitochondrial disease is associated with defective NFU1 function in the maturation of a subset of mitochondrial Fe-S proteins. *Am. J. Hum. Genet.* **89**, 656–667
31. Gao, H., Subramanian, S., Couturier, J., Naik, S. G., Kim, S.-K., Leustek, T., Knaff, D. B., Wu, H.-C., Vignols, F., Huynh, B. H., Rouhier, N., and Johnson, M. K. (2013) Arabidopsis thaliana Nfu2 accommodates [2Fe-2S] or [4Fe-4S] clusters and is competent for in vitro maturation of chloroplast [2Fe-2S] and [4Fe-4S] cluster-containing proteins.

Biochemistry (Mosc.). **52**, 6633–6645

32. Boutigny, S., Saini, A., Baidoo, E. E. K., Yeung, N., Keasling, J. D., and Butland, G. (2013) Physical and functional interactions of a monothiol glutaredoxin and an iron sulfur cluster carrier protein with the sulfur-donating radical S-adenosyl-L-methionine enzyme MiaB. *J. Biol. Chem.* **288**, 14200–14211
33. Melber, A., Na, U., Vashisht, A., Weiler, B. D., Lill, R., Wohlschlegel, J. A., and Winge, D. R. (2016) Role of Nfu1 and Bol3 in iron-sulfur cluster transfer to mitochondrial clients. *eLife*. 10.7554/eLife.15991
34. Flint, D. H., Smyk-Randall, E., Tuminello, J. F., Draczynska-Lusiak, B., and Brown, O. R. (1993) The inactivation of dihydroxy-acid dehydratase in *Escherichia coli* treated with hyperbaric oxygen occurs because of the destruction of its Fe-S cluster, but the enzyme remains in the cell in a form that can be reactivated. *J. Biol. Chem.* **268**, 25547–25552
35. Alhebshi, A., Sideri, T. C., Holland, S. L., and Avery, S. V. (2012) The essential iron-sulfur protein Rli1 is an important target accounting for inhibition of cell growth by reactive oxygen species. *Mol. Biol. Cell.* **23**, 3582–3590
36. Rivasseau, C., Seemann, M., Boisson, A.-M., Streb, P., Gout, E., Douce, R., Rohmer, M., and Bligny, R. (2009) Accumulation of 2-C-methyl-D-erythritol 2,4-cyclodiphosphate in illuminated plant leaves at supraoptimal temperatures reveals a bottleneck of the prokaryotic methylerythritol 4-phosphate pathway of isoprenoid biosynthesis. *Plant Cell Environ.* **32**, 82–92
37. Vinella, D., Loiseau, L., Ollagnier de Choudens, S., Fontecave, M., and Barras, F. (2013) In vivo [Fe-S] cluster acquisition by IscR and NsrR, two stress regulators in *Escherichia coli*. *Mol. Microbiol.* **87**, 493–508
38. Wolff, M., Seemann, M., Tse Sum Bui, B., Frapart, Y., Tritsch, D., Garcia Estrabot, A., Rodríguez-Concepción, M., Boronat, A., Marquet, A., and Rohmer, M. (2003) Isoprenoid biosynthesis via the methylerythritol phosphate pathway: the (E)-4-hydroxy-3-methylbut-2-enyl diphosphate reductase (LytB/IspH) from *Escherichia coli* is a [4Fe-4S] protein. *FEBS Lett.* **541**, 115–120
39. Gräwert, T., Kaiser, J., Zepeck, F., Laupitz, R., Hecht, S., Amslinger, S., Schramek, N., Schleicher, E., Weber, S., Haslbeck, M., Buchner, J., Rieder, C., Arigoni, D., Bacher, A., Eisenreich, W., and Rohdich, F. (2004) IspH protein of *Escherichia coli*: studies on iron-sulfur cluster implementation and catalysis. *J. Am. Chem. Soc.* **126**, 12847–12855
40. Py, B., Gerez, C., Angelini, S., Planel, R., Vinella, D., Loiseau, L., Talla, E., Brochier-Armanet, C., Garcia Serres, R., Latour, J.-M., Ollagnier-de Choudens, S., Fontecave, M., and Barras, F. (2012) Molecular organization, biochemical function, cellular role and evolution of NfuA, an atypical Fe-S carrier. *Mol. Microbiol.* **86**, 155–171
41. Beilschmidt, L. K., and Puccio, H. M. (2014) Mammalian Fe-S cluster biogenesis and its implication in disease. *Biochimie.* **100**, 48–60
42. Ezraty, B., Vergnes, A., Banzhaf, M., Duverger, Y., Huguenot, A., Brochado, A. R., Su, S.-Y., Espinosa, L., Loiseau, L., Py, B., Typas, A., and Barras, F. (2013) Fe-S cluster biosynthesis controls uptake of aminoglycosides in a ROS-less death pathway. *Science.* **340**, 1583–1587
43. Gelling, C., Dawes, I. W., Richhardt, N., Lill, R., and Mühlenhoff, U. (2008) Mitochondrial Iba57p is required for Fe/S cluster formation on aconitase and activation of radical SAM enzymes. *Mol. Cell. Biol.* **28**, 1851–1861
44. Mühlenhoff, U., Richter, N., Pines, O., Pierik, A. J., and Lill, R. (2011) Specialized function of yeast Isa1 and Isa2 proteins in the maturation of mitochondrial [4Fe-4S] proteins. *J. Biol. Chem.* **286**, 41205–41216

45. Brancaccio, D., Gallo, A., Mikolajczyk, M., Zovo, K., Palumaa, P., Novellino, E., Piccioli, M., Ciofi-Baffoni, S., and Banci, L. (2014) Formation of [4Fe-4S] clusters in the mitochondrial iron-sulfur cluster assembly machinery. *J. Am. Chem. Soc.* **136**, 16240–16250
46. Beilschmidt, L. K., Ollagnier de Choudens, S., Fournier, M., Sanakis, I., Hograindleur, M.-A., Clémancey, M., Blondin, G., Schmucker, S., Eisenmann, A., Weiss, A., Koebel, P., Messaddeq, N., Puccio, H., and Martelli, A. (2017) ISCA1 is essential for mitochondrial Fe₄S₄ biogenesis in vivo. *Nat. Commun.* **8**, 15124
47. Schilke, B., Voisine, C., Beinert, H., and Craig, E. (1999) Evidence for a conserved system for iron metabolism in the mitochondria of *Saccharomyces cerevisiae*. *Proc. Natl. Acad. Sci. U. S. A.* **96**, 10206–10211
48. Baba, T., Ara, T., Hasegawa, M., Takai, Y., Okumura, Y., Baba, M., Datsenko, K. A., Tomita, M., Wanner, B. L., and Mori, H. (2006) Construction of *Escherichia coli* K-12 in-frame, single-gene knockout mutants: the Keio collection. *Mol. Syst. Biol.* **2**, 2006.0008
49. Ollagnier-de Choudens, S., Nachin, L., Sanakis, Y., Loiseau, L., Barras, F., and Fontecave, M. (2003) SufA from *Erwinia chrysanthemi*. Characterization of a scaffold protein required for iron-sulfur cluster assembly. *J. Biol. Chem.* **278**, 17993–18001
50. Jordan, P. A., Tang, Y., Bradbury, A. J., Thomson, A. J., and Guest, J. R. (1999) Biochemical and spectroscopic characterization of *Escherichia coli* aconitases (AcnA and AcnB). *Biochem. J.* **344 Pt 3**, 739–746
51. Karimova, G., Pidoux, J., Ullmann, A., and Ladant, D. (1998) A bacterial two-hybrid system based on a reconstituted signal transduction pathway. *Proc. Natl. Acad. Sci. U. S. A.* **95**, 5752–5756
52. Ollagnier-de Choudens, S., Nachin, L., Sanakis, Y., Loiseau, L., Barras, F., and Fontecave, M. (2003) SufA from *Erwinia chrysanthemi*. Characterization of a scaffold protein required for iron-sulfur cluster assembly. *J. Biol. Chem.* **278**, 17993–18001
53. Beinert, H. (1983) Semi-micro methods for analysis of labile sulfide and of labile sulfide plus sulfane sulfur in unusually stable iron-sulfur proteins. *Anal. Biochem.* **131**, 373–378
54. Fish, W. W. (1988) Rapid colorimetric micromethod for the quantitation of complexed iron in biological samples. *Methods Enzymol.* **158**, 357–364
55. Vogel, A. (1989) Textbook of Quantitative Chemical Analysis
56. Gardner, P. R., and Fridovich, I. (1992) Inactivation-reactivation of aconitase in *Escherichia coli*. A sensitive measure of superoxide radical. *J. Biol. Chem.* **267**, 8757–8763
57. Seaver, L. C., and Imlay, J. A. (2004) Are respiratory enzymes the primary sources of intracellular hydrogen peroxide? *J. Biol. Chem.* **279**, 48742–48750
58. Guzman, L. M., Belin, D., Carson, M. J., and Beckwith, J. (1995) Tight regulation, modulation, and high-level expression by vectors containing the arabinose PBAD promoter. *J. Bacteriol.* **177**, 4121–4130

Table 1. Strains and plasmids used in this study

Strain	Relevant phenotype	Reference or source
MG1655	Parental strain	Laboratory collection
$\Delta nfuA$	MG1655 $\Delta nfuA::kan$ cured with pCP20	(40)
Wt MVA+	MG1655 derivative carrying the mevalonate (MVA) pathway genes in the chromosome	(17)
$\Delta nfuA$ MVA+	MG1655 $\Delta nfuA$ derivative carrying the MVA pathway genes	(40)
LL401	MG1655 derivative, <i>erpA</i> placed under control of the pBAD promoter of specRExBAD cassette	(17)
BP721	LL401 derivative carrying $\Delta acnA::kan$	This study
BTH101	F- <i>cyo-99 araD139 galE15 galK16 rpsL1</i> (Str ^R) <i>hsdR2 McrA1 McrB1</i>	(51)
Plasmid		
pKT25	p15A, Plac, T25 domain (CyaA 1-224 aa)	(51)
pT25-IscA	pKT25 expressing T25-IscA hybrid protein	This study
pT25-SufA	pKT25 expressing T25-SufA hybrid protein	This study
pT25-ErpA	pKT25 expressing T25-ErpA hybrid protein	This study
pT25-NfuA	pKT25 expressing T25-NfuA hybrid protein	(40)
pT25-ATC*	pKT25 expressing the N-terminal domain of NfuA (ATC*) fused to the T25 polypeptide	(40)
pT25-Nfu	pKT25 expressing the N-terminal domain of NfuA (ATC*) fused to the T25 polypeptide	(40)
pUT18C	AmpR, Col E1 ori, Plac, T18 domain (CyaA 225-399 aa)	(51)
pT18-NfuA	pUT18C expressing T18-NfuA hybrid protein	(40)
pT18-IspH	pUT18C expressing T18-IspH hybrid protein	This study
pBAD24	Cloning vector	(58)
pBAD- <i>nfuA</i>	pBAD derivative, <i>nfuA</i> placed under control of the pBAD promoter	(25)
pLAI-A (pBAD- <i>iscA</i>)	pBAD derivative, <i>iscA</i> placed under control of the pBAD promoter	(16)
pLAS-A (pBAD- <i>sufA</i>)	pBAD derivative, <i>sufA</i> placed under control of the pBAD promoter	(16)
pLAE-A (pBAD- <i>erpA</i>)	pBAD derivative, <i>erpA</i> placed under control of the pBAD promoter	(16)
pUC18	Cloning vector	In vitrogen
pUC- <i>erpA</i>	pUC18 derivative carrying <i>erpA</i>	(17)
pUC- <i>nfuA</i>	pUC18 derivative carrying <i>nfuA</i>	(25)

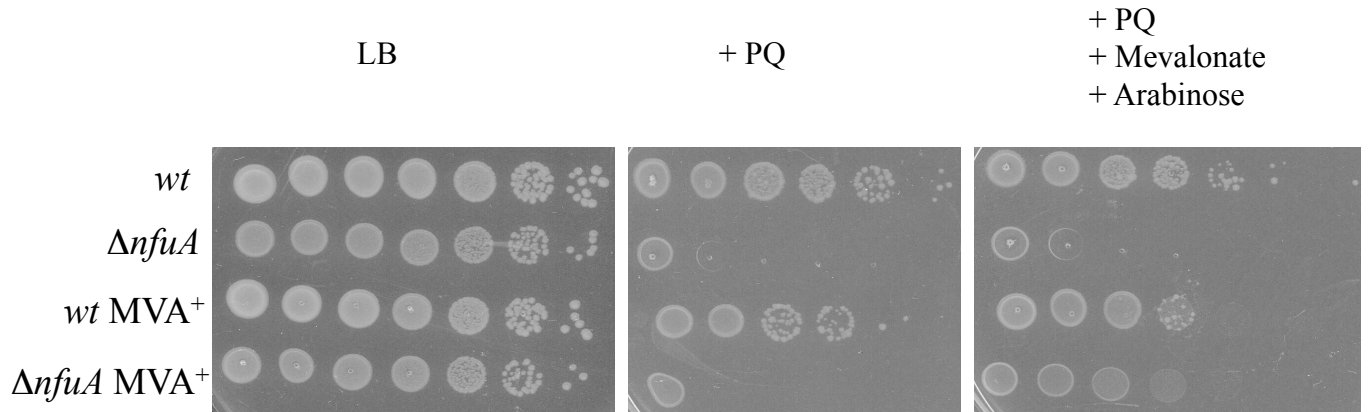


Figure 1. NfuA is required for IPP biosynthesis in *E. coli* during oxidative stress. Wild-type (MG1655), $\Delta nfuA$, *wt* MVA⁺ and $\Delta nfuA$ MVA⁺ strains were grown overnight at 37 °C in LB medium. Cultures were diluted in sterile PBS, and 5 μ L were directly spotted onto LB medium plate, LB medium plate supplemented with 100 μ M paraquat (PQ), and containing the mevalonate (MVA) pathway inducer L-arabinose (0.2%) and the MVA substrate (mevalonate, 1 mM). Growth was analyzed after overnight incubation at 37 °C. Each spot represents a 10-fold serial dilution.

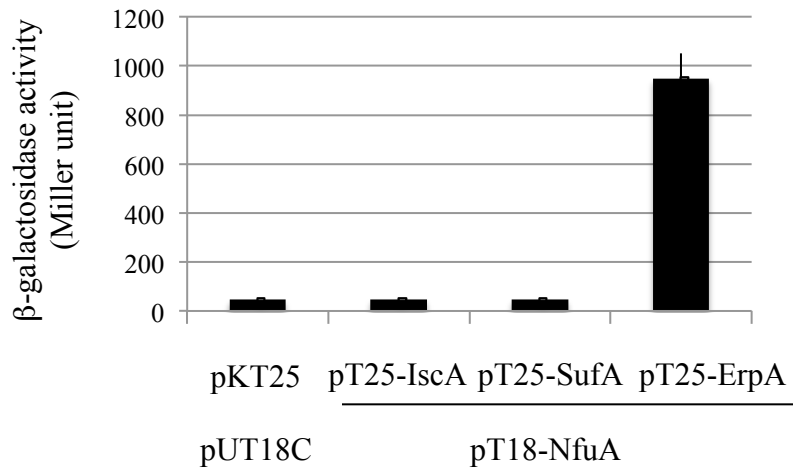
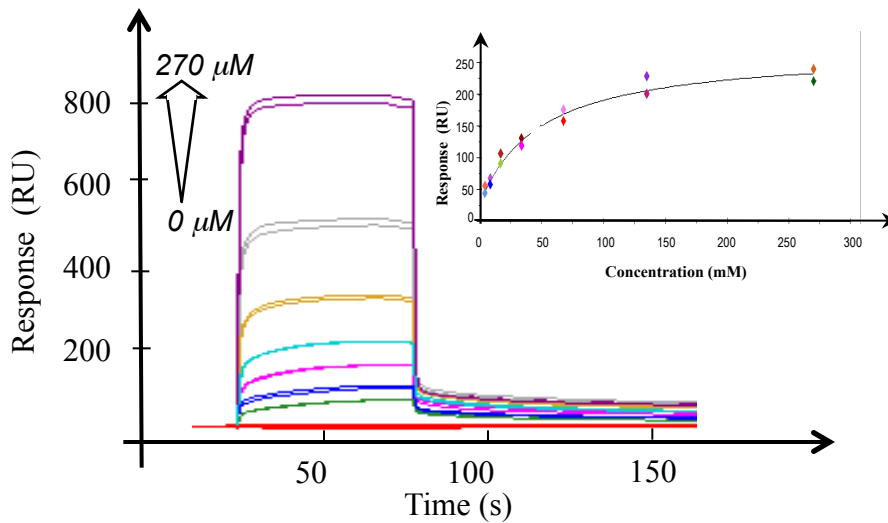
A**B**

Figure 2. NfuA interacts with ErpA. Study of the interaction between NfuA and ErpA using bacterial two-hybrid (A) and surface plasmon resonance (B) analyses. (A) The β -galactosidase activity of the adenylate cyclase-deficient BTH101 strains carrying the indicated plasmids was determined and expressed in Miller unit. (B) Serially diluted ErpA (red: 0; green: 4.2 μ M; blue: 8.44 μ M; pink: 16.88 μ M; cyan: 33.75 μ M; yellow: 67.5 μ M; grey: 135 μ M; purple: 270 μ M) in HBS buffer was injected at a flow rate of 10 μ L/min through flow cells with the immobilized NfuA on a CM5 chip. Inset: affinity curve of ErpA flowing on NfuA. The experiments were run in duplicate.

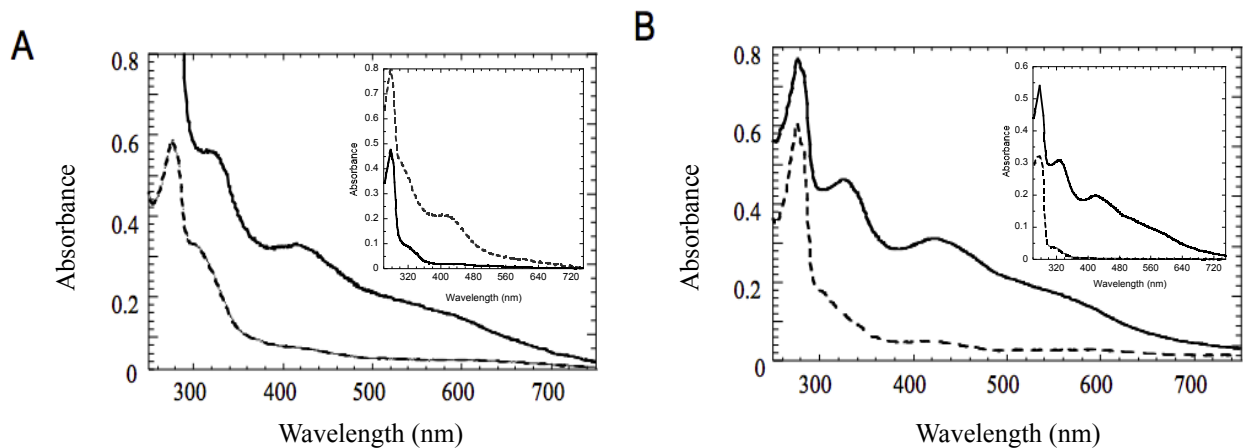
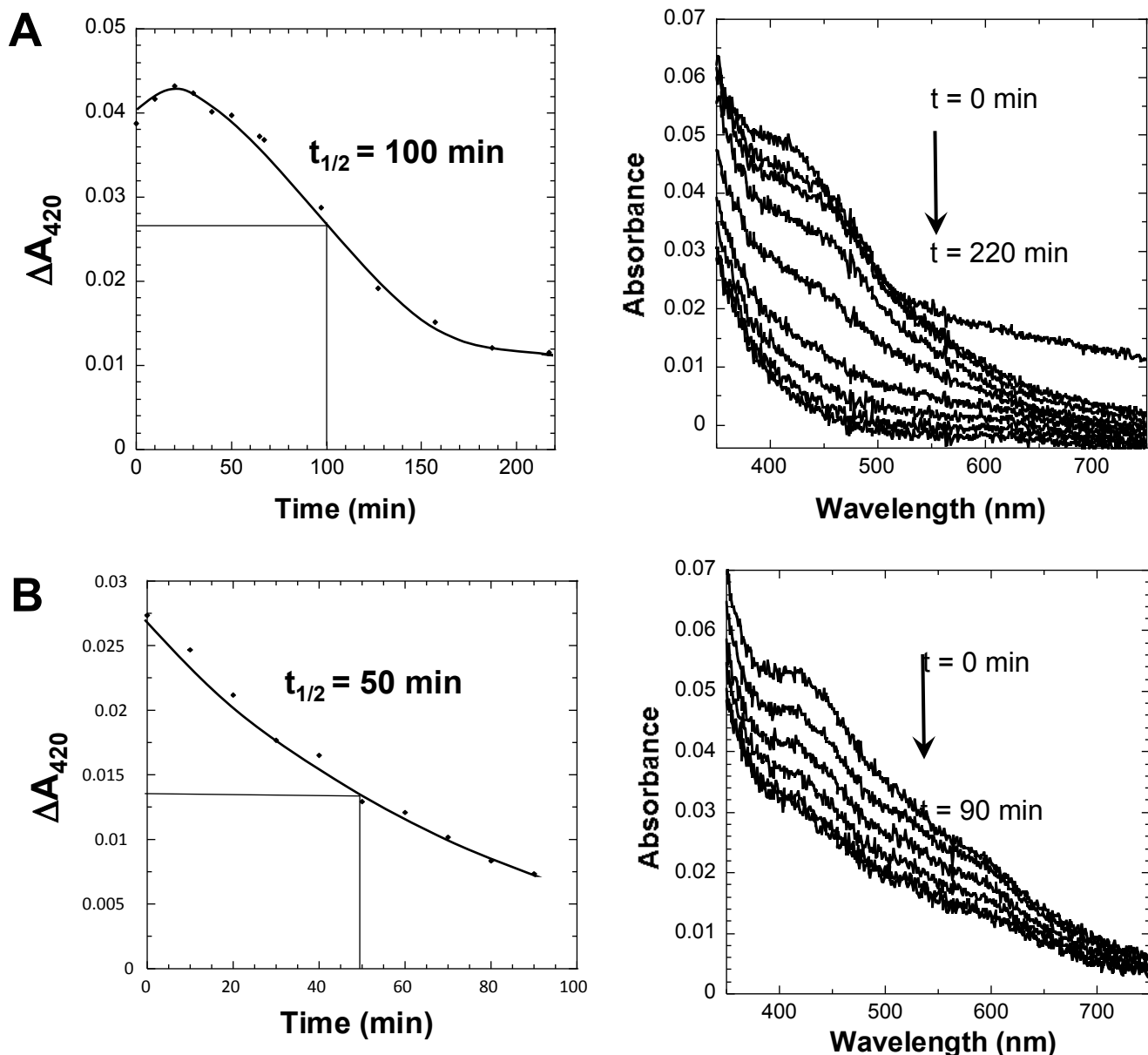


Figure 3. Unidirectional Fe-S cluster transfer between NfuA and ErpA. (A) The apo-ErpA (150 μ M) was first pre-reduced with 5 mM DTT. After removal of the latter, holo-NfuA-his, the Fe-S cluster donor, and the apo-ErpA proteins were mixed together in 0.1 M Tris-HCl pH 8, 50 mM KCl in a molar ratio calculated to give 1 iron and 1 sulfur atoms per ErpA monomer. After separation on the Ni-NTA column, the UV-vis spectra of the wash fraction containing ErpA (solid line) and the eluate fraction (dashed line) containing NfuA-his were recorded. (B) For transfer from holo-ErpA to apo-NfuA-his, apo-NfuA-his (150 μ M) was mixed together with the holo-ErpA in a molar ratio calculated to give 2 iron and 2 sulfur atoms per monomer NfuA in buffer 0.1 M Tris-HCl pH 8, 50 mM KCl, 5 mM DTT. After removal of DTT and separation onto a Ni-NTA column, the UV-vis spectra of the wash fraction containing ErpA (solid line) and the eluate fraction (dashed line) containing NfuA-his were recorded. The insets show holo- and apo-proteins, ErpA (solid line) and NfuA (dashed line) before the reaction.



C

Protein	$t_{1/2}$ (min)
ErpA _{rec}	54 +/- 4
SufA _{rec}	55 +/- 7
IscA _{rec}	45 +/- 3
NfuA _{rec}	100 +/- 10

Figure 4. NfuA has a more stable Fe-S cluster than ErpA. NfuA (A) and ErpA (B) were reconstituted in the glove box and the excess of iron and sulfur taken off in a microbiospin column. The reconstituted proteins were injected in a cuvette containing 100 μL of oxygenated Tris buffer (28.4 nmol O_2) to give a ratio 1/20 for (amount Fe)/ O_2 . UV-vis spectra at various time points (right panel) (0-220 min for NfuA, and 0-90 min for ErpA); representation of the decay of Abs_{420} as function of time ($\Delta\text{Abs}_{420} = \text{Abs}_{420} \text{ sample} - \text{Abs}_{420} \text{ blank}$) (left panel). (C) Half-life of the Fe-S cluster of the indicated reconstituted proteins in oxygenated Tris buffer. In these experiments SufA initially contained 0.9 +/- 0.1 Fe and 0.9 +/- 0.2 S/monomer and IscA contained 1 +/- 0.2 Fe and 0.8 +/- 0.1 S/monomer. The experiments were run in duplicate.

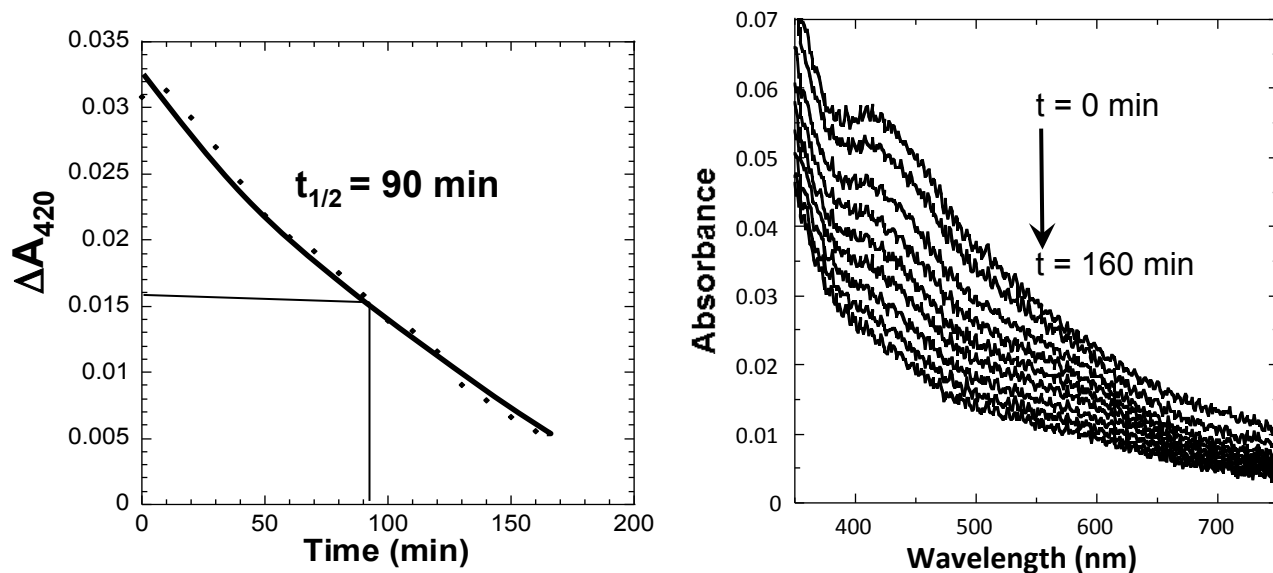


Figure 5. NfuA stabilizes the Fe-S cluster of ErpA. Equimolar amount of apo-NfuA was added to reconstituted ErpA and the mixture was incubated for one hour inside the glove box before being injected in a cuvette containing 100 μL of oxygenated Tris buffer (28,4 nmol O_2) to give a ratio 1/20 for (amount Fe)/ O_2 . UV-vis spectra every 20 min (0-160 min) (right panel); representation of the decay of Abs_{416} as function of time ($\Delta\text{Abs}_{420} = \text{Abs}_{420} \text{ sample} - \text{Abs}_{420} \text{ blank}$) (left panel).

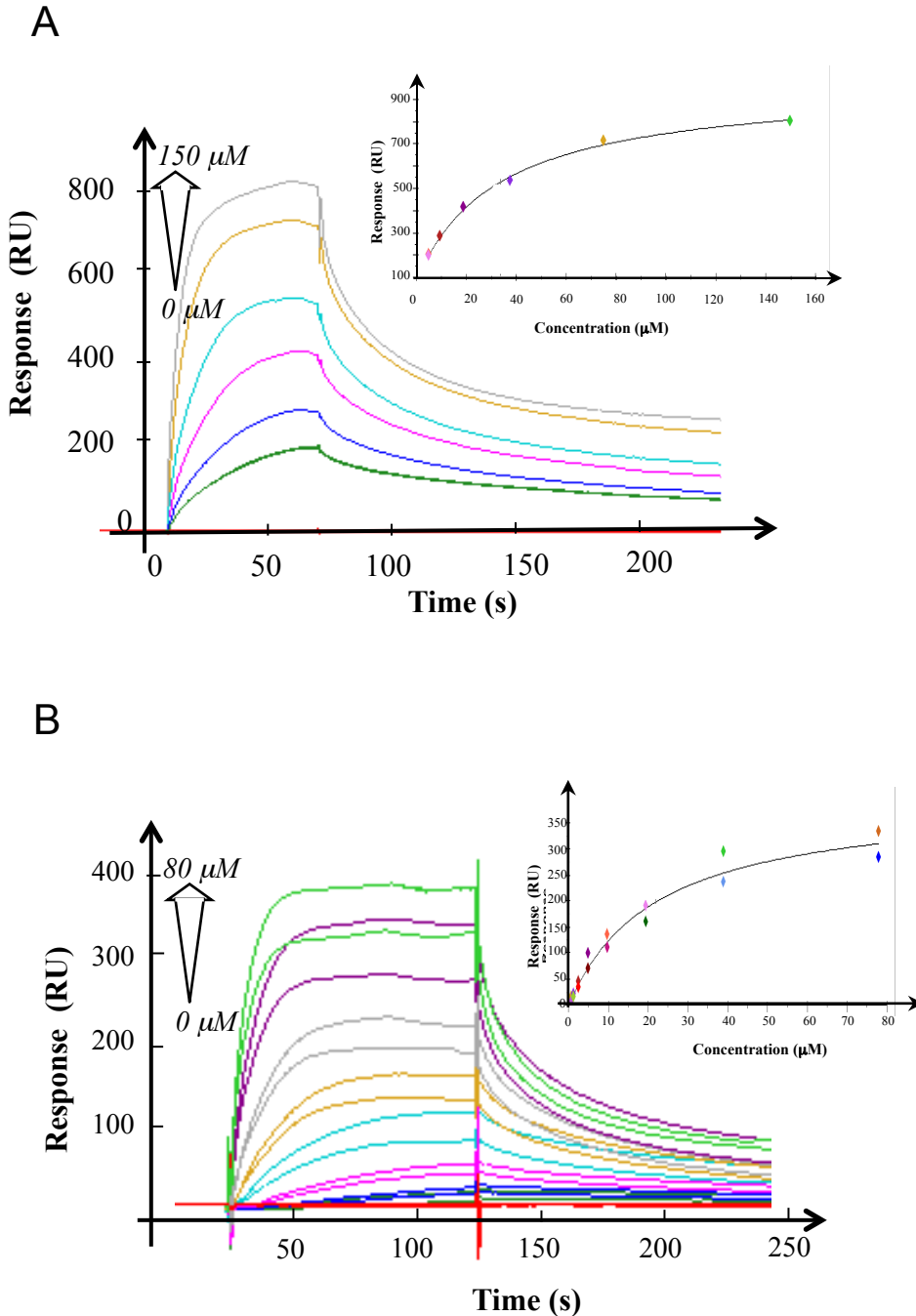


Figure 6. IspG interacts with NfuA and ErpA. Surface plasmon resonance analysis of IspG to the Fe-S clusters carrier proteins NfuA and ErpA. (A) Serially diluted IspG (red: 0; green: 4.69 μM ; blue: 9.38 μM ; pink: 18.75 μM ; cyan: 37.5 μM ; yellow: 75 μM ; grey: 150 μM) in HBS buffer was injected at a flow rate of 10 $\mu\text{l}/\text{min}$ through flow cells with the immobilized NfuA on a CM5 chip. The injection of IspG (4.69 μM) was run in duplicate. (B) Serially diluted IspG (red: 0; green: 0.61 μM blue: 1.21 μM ; pink: 2.44 μM ; cyan: 4.88 μM ; yellow: 9.75 μM ; grey: 19.5 μM ; purple: 39 μM ; light green 78 μM) in Tris buffer was injected at a flow rate of 10 $\mu\text{L}/\text{min}$ through flow cells with the immobilized ErpA on a CM5 chip. The experiments were run in duplicate.

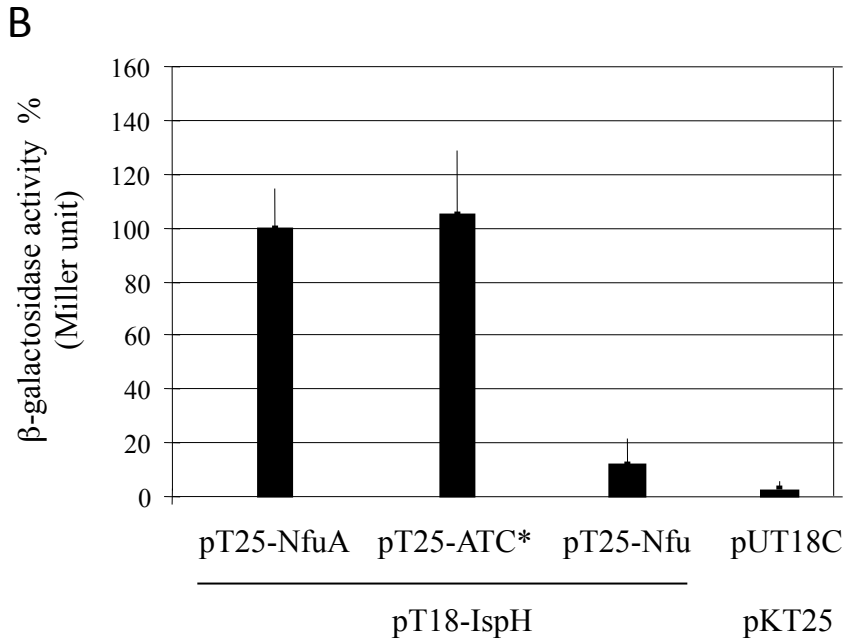
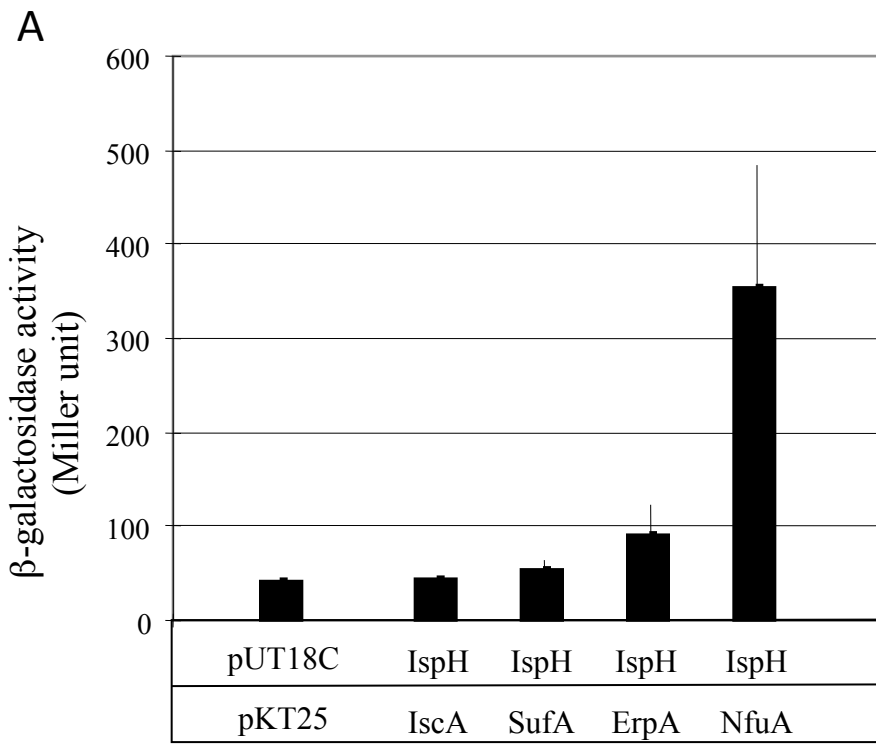


Figure 7. IspH interacts with NfuA. Study of the interaction between IspH and NfuA using bacterial two-hybrid. (A) The β -galactosidase activity of the adenylate cyclase-deficient BTH101 strains carrying the indicated plasmids was determined and expressed in Miller unit. (B) The N-terminal ATC* domain of NfuA interacts with IspH. The β -galactosidase activities of the BTH101 strain carrying the pT18-IspH plasmid together with the pT25-NfuA (full length NfuA), the pT25-ATC* (NfuA N-terminal domain), and the pT25-Nfu (NfuA C-terminal domain) plasmids were determined (Miller unit) and expressed as a percentage, the values obtained with the full-length NfuA set to 100%. The pUT18C and pKT25 plasmids are control empty vectors. The experiments were run in triplicate and the standard errors are shown.

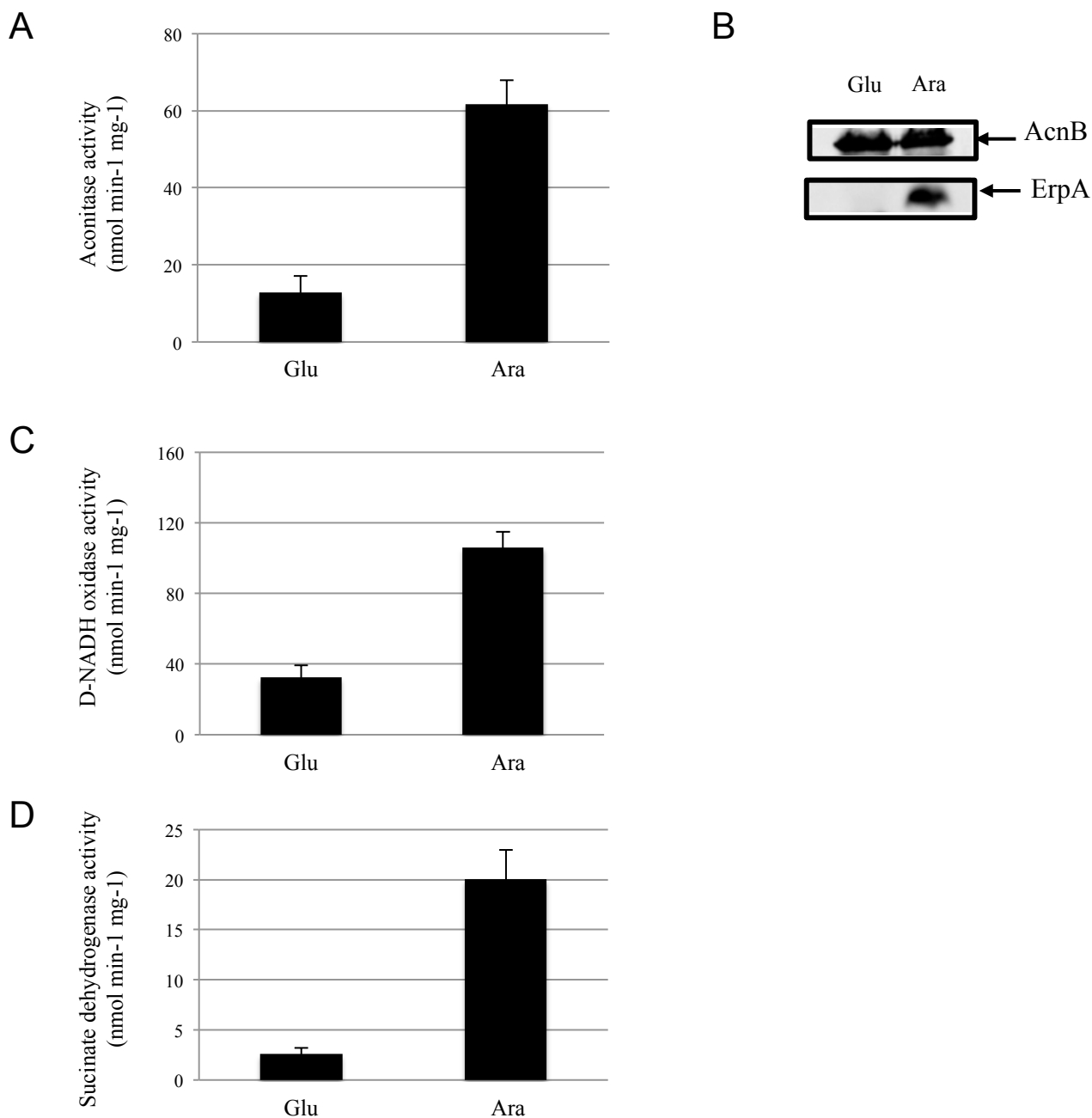


Figure 8. Aconitase B and respiratory complexes I and II activities are compromised in ErpA depleted cells. Strains were grown ON in LB supplemented with arabinose. Fresh LB medium with 0,2% of glucose (Glu) or arabinose (Ara) was inoculated. Samples were taken and analyzed when cells reached late-exponential phase (3,5-4 hours of growth). A) Aconitase activity was assayed using the *ara_p::erpA ΔacnA* strain (BP721). B) Immunoblot analysis was performed, on glucose (Glu) or arabinose (Ara) grown cells of the BP721 strain using antibodies raised against AcnB (top panel) and ErpA (bottom panel); identical amount of total proteins were loaded. D-NADH oxidase activity (C) and succinate dehydrogenase (D) activities were assayed from the LL401 strain (*ara_p::erpA*) strains. The experiments were run in triplicate and the standard errors are shown.

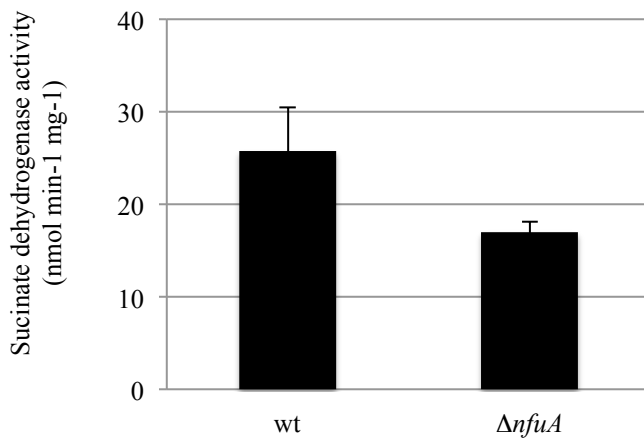


Figure 9. NfuA is required for respiratory complex II activity. Effect of a $\Delta nfuA$ mutation on SDH activity. Succinate dehydrogenase activity was assayed from MG1655 (wt) and MG1655 $\Delta nfuA$. The experiments were run at least in triplicate and the standard errors are shown.

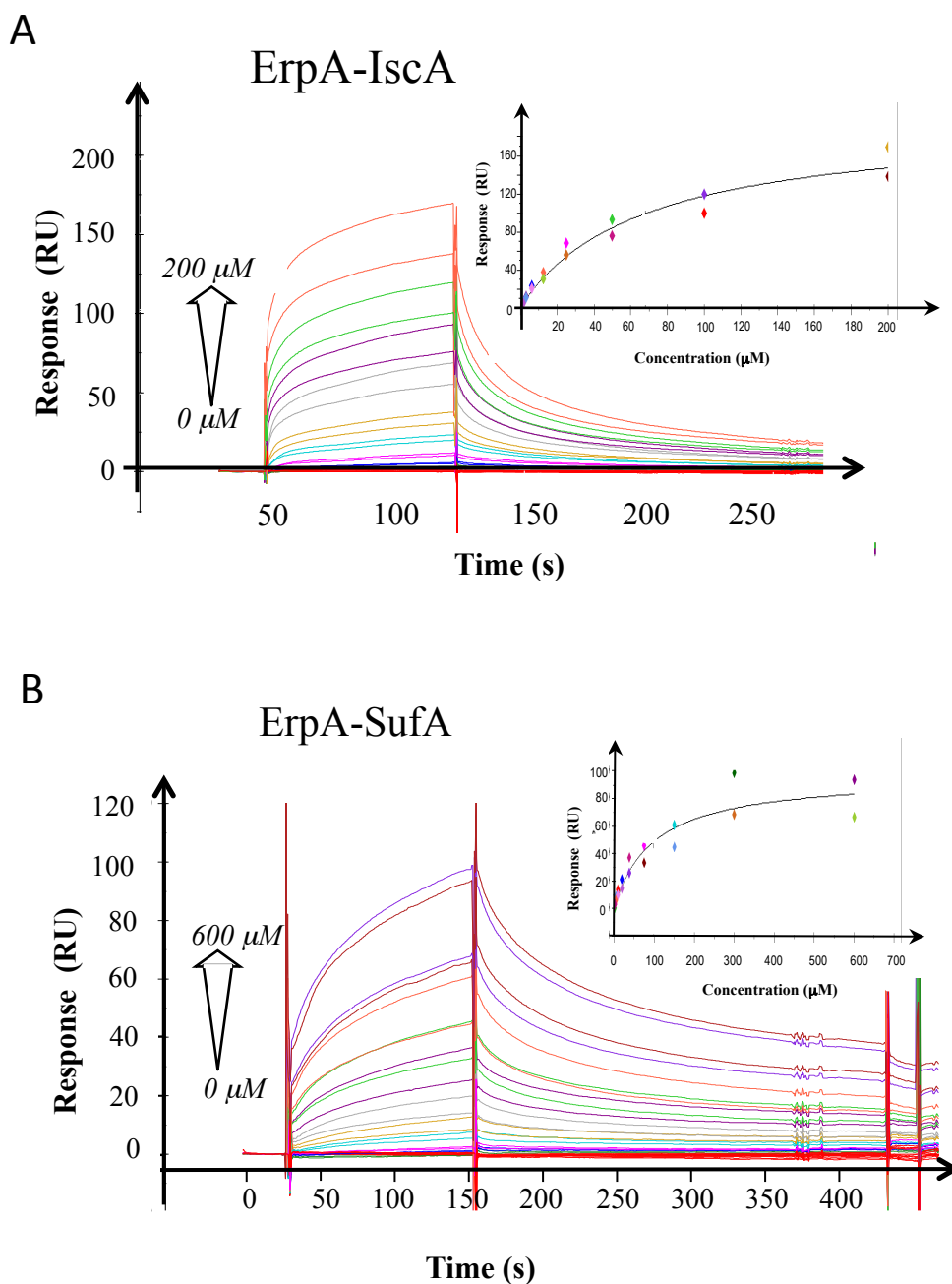


Figure 10. ErpA interacts with IscA and SufA. In surface plasmon resonance experiments, serially diluted IscA (0-200 μ M) (A) and SufA (0-600 μ M), in Tris buffer, were injected at a flow rate of 10 μ l/min through flow cells with the immobilized ErpA on a CM5 chip. The experiment was run in duplicate.

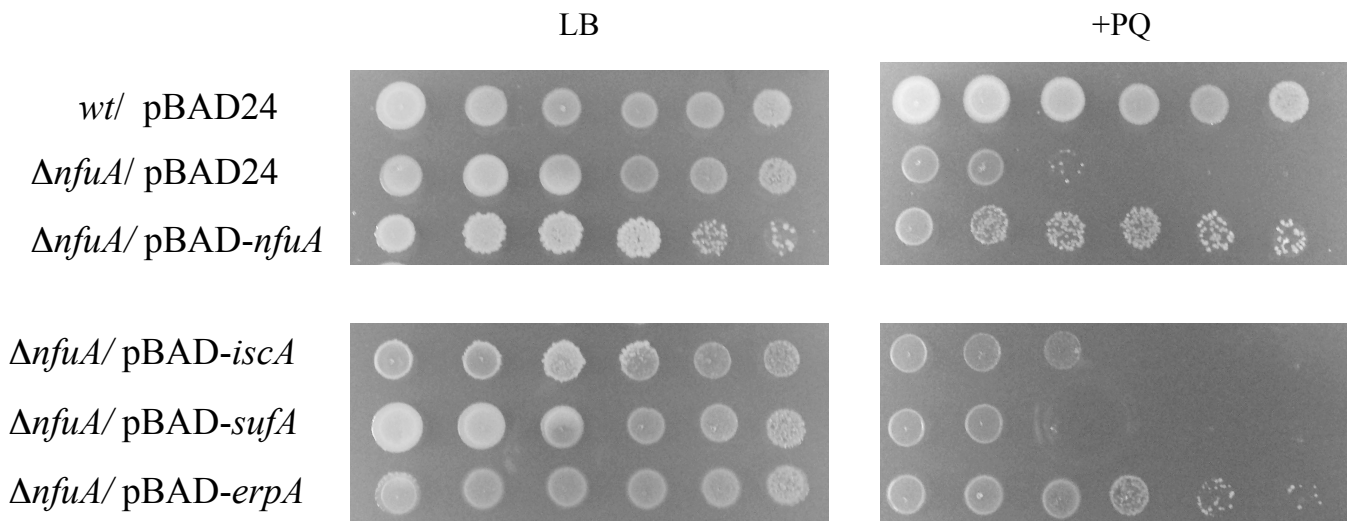


Figure 11. Multicopy suppression of the *nfuA* growth defect during oxidative stress, by *erpA*. Wild-type (MG1655), and Δ *nfuA* strains transformed with the pBAD24 control vector, the pBAD-*nfuA*, pBAD-*iscA*, pBAD-*sufA*, or pBAD-*erpA* plasmids, were spotted on LB medium plates containing ampicillin and arabinose, supplemented (right) or not (left) with 100 μ M paraquat. Growth was analyzed after overnight incubation at 37 °C. Each spot represents a 10-fold serial dilution.

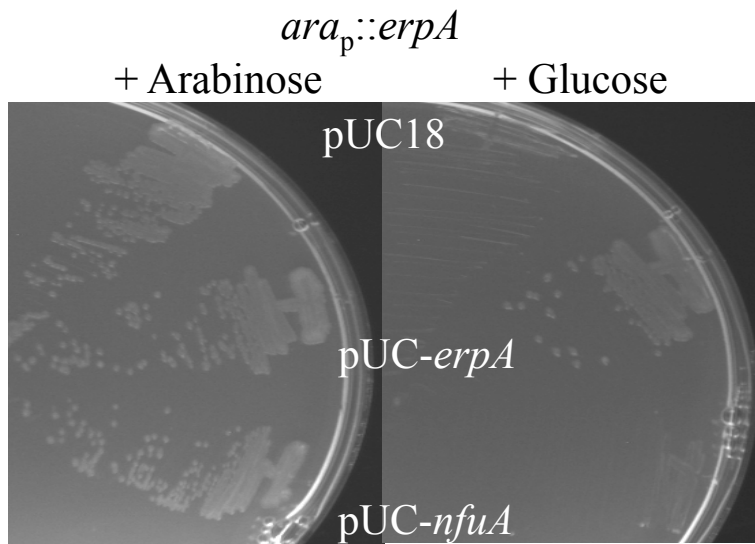


Figure 12. NfuA does not suppress lethality of the conditional *erpA* mutant. The LL401(*ara_p::erpA*)/pUC18 (top), LL401(*ara_p::erpA*)/pUC-*erpA* (middle) and LL401(*ara_p::erpA*)/pUC-*nfuA* (bottom) strains were grown on LB medium plates supplemented with 0.2% arabinose (left) or 0.2% glucose (right).

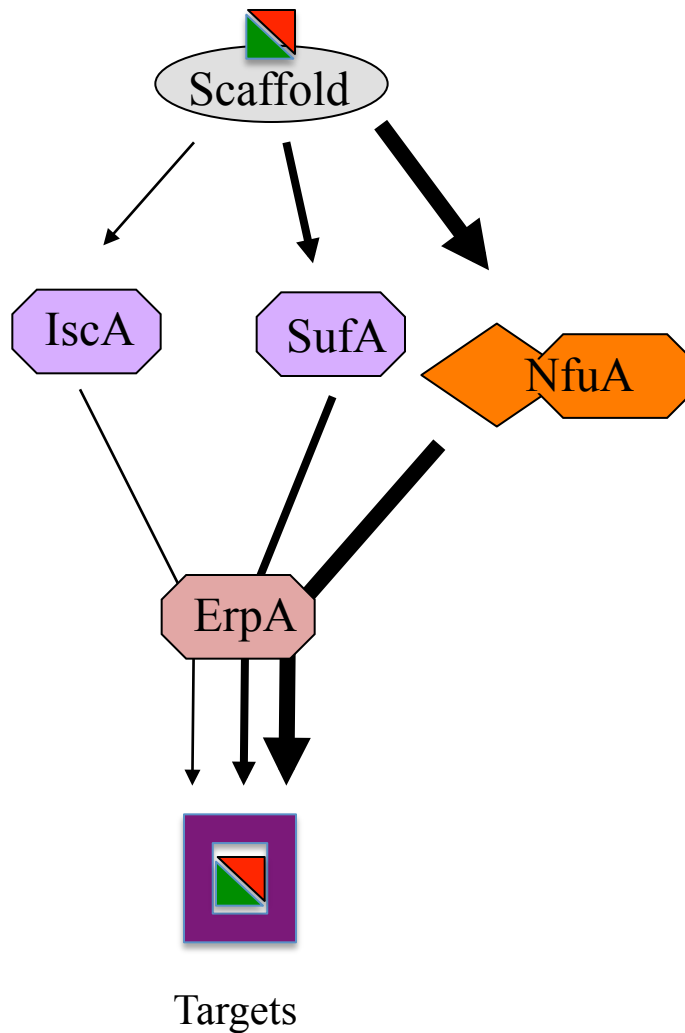


Figure 13. Working model of the *E. coli* Fe-S delivery step. Arrows represent the routes (i.e. the carriers used, IscA, SufA, ErpA, NfuA) to deliver the Fe-S clusters (green/red triangles) from the scaffold to the target proteins. The thickness of the arrows increases with the level of ROS met by the bacterium.